

N72-11980

NASA TECHNICAL  
MEMORANDUM



NASA TM X-2432

NASA TM X-2432

CASE FILE  
COPY

A PARAMETRIC STUDY OF MOTOR  
STARTING FOR A 2- TO 10-KILOWATT  
BRAYTON POWER SYSTEM

by Dennis A. Cantoni

Lewis Research Center  
Cleveland, Ohio 44135

NATIONAL AERONAUTICS AND SPACE ADMINISTRATION • WASHINGTON, D. C. • NOVEMBER 1971

1 Report No  NASA TM X-2432	2 Government Accession No	3 Recipient's Catalog No	
4 Title and Subtitle  A PARAMETRIC STUDY OF MOTOR STARTING FOR A 2- TO 10-KILOWATT BRAYTON POWER SYSTEM		5. Report Date  November 1971	6 Performing Organization Code
7 Author(s)  Dennis A. Cantoni		8 Performing Organization Report No.  E-6548	
9 Performing Organization Name and Address  Lewis Research Center National Aeronautics and Space Administration Cleveland, Ohio 44135		10 Work Unit No  112-27	11 Contract or Grant No
12 Sponsoring Agency Name and Address  National Aeronautics and Space Administration Washington, D.C. 20546		13 Type of Report and Period Covered  Technical Memorandum	14 Sponsoring Agency Code
15 Supplementary Notes			
16 Abstract  A study of the motor starting of a Brayton cycle power system was conducted to provide estimates of system sensitivity to several controllable parameters. These sensitivity estimates were used as a basis for selection of an optimum motor-start scheme to be implemented on the 2- to 10-kilowatt Brayton power system designed and presently under test at the NASA Lewis Research Center. The studies were conducted with an analog simulation of the Brayton power system and covered a range of frequencies from 400 Hz (33 percent design) to 1200 Hz (design), voltage-to-frequency ratios of 0.050 (50 percent design) to 0.100 (design), turbine-inlet temperatures of 800 K (1440° R, 70 percent design) to 1140 K (2060° R, design), and prestart pressure levels of 10.0 N/cm <sup>2</sup> abs (14.5 psia) to 20.0 N/cm <sup>2</sup> abs (29.0 psia). These studies have shown the effect of selected system variables on motor starting. The final selection of motor-start variables can therefore be made on the bases of motor-start inverter complexity, battery size and weight, desired steady-state pressure level after startup, and other operational limitations. In general, the study showed the time required for motor starting to be inversely proportional to motor frequency, voltage, turbine-inlet temperature, and pressure level. An increase in any of these parameters decreases startup time.			
17. Key Words (Suggested by Author(s))  Space power Power systems Simulation Startup of power systems		18 Distribution Statement  Unclassified - unlimited	
19 Security Classif (of this report)  Unclassified	20 Security Classif (of this page)  Unclassified	21 No of Pages  20	22 Price*  \$3.00

<sup>\*</sup> For sale by the National Technical Information Service, Springfield, Virginia 22151

# A PARAMETRIC STUDY OF MOTOR STARTING FOR A 2- TO 10-KILOWATT BRAYTON POWER SYSTEM

by Dennis A. Cantoni

Lewis Research Center

## SUMMARY

A study of the motor starting of a Brayton cycle power system was conducted to provide estimates of system sensitivity to several controllable parameters. These sensitivity estimates were used as a basis for selection of an optimum motor-start scheme to be implemented on the 2- to 10-kilowatt Brayton power system designed and presently under test at the NASA Lewis Research Center.

The studies were conducted with an analog simulation of the Brayton power system and covered a range of frequencies from 400 Hz (33 percent design) to 1200 Hz (design), voltage-to-frequency ratios of 0.050 (50 percent design) to 0.100 (design), turbine-inlet temperatures of 800 K ( $1440^{\circ}$  R, 70 percent design) to 1140 K ( $2060^{\circ}$  R, design), and prestart pressure levels of  $10.0 \text{ N/cm}^2 \text{ abs}$  (14.5 psia) to  $20.0 \text{ N/cm}^2 \text{ abs}$  (29.0 psia).

These studies have shown the effect of selected system variables on motor starting. The final selection of motor-start variables can therefore be made on the bases of motor-start inverter complexity, battery size and weight, desired steady-state pressure level after startup, and other operational limitations.

In general, the study showed the time required for motor starting to be inversely proportional to motor frequency, voltage, turbine-inlet temperature, and pressure level. An increase in any of these parameters decreases startup time.

## INTRODUCTION

The NASA Lewis Research Center has designed and is testing a 2- to 10-kilowatt, closed-loop Brayton cycle system for electric power generation in space. The system consists of a heat-source subsystem, a power-conversion subsystem, and a heat-rejection subsystem. The power-conversion subsystem is designed to be used with various heat sources. In the power-conversion subsystem, hot gas drives a turbine

which is coupled to a compressor and an alternator. This single rotational component has been designated the Brayton Rotating Unit (BRU). Additional power-conversion hardware includes a gas-to-gas recuperator, a gas-to-liquid heat exchanger, a gas-management subsystem, and an electrical subsystem. A more detailed description of the Brayton system can be found in reference 1.

Two methods of starting the Brayton system are being designed into the system: (1) motoring the alternator from an auxiliary source; and (2) powering the turbine by forced gas injection. The gas-injection method of startup has already been tested and is reported in reference 2. Initial motor-start tests are reported in reference 3.

The purpose of this computer study was to examine the effects of system variables on motor starting the closed-loop Brayton system to provide a basis for optimizing the motor-start method. Reported herein are the computer-analysis results showing the effects of various system parameters. The studies were made for turbine-inlet temperatures of 800 K ( $1440^{\circ}$  R) to 1140 K ( $2060^{\circ}$  R), system-prestart pressure levels of 10.0 to 20.0 N/cm<sup>2</sup> abs (14.5 to 29.0 psia), motoring frequencies of 400 to 1200 Hz, and applied-voltage-to-frequency ratios of 0.05 to 0.10.

## SYSTEM DESCRIPTION

A schematic diagram of the Brayton power system is shown in figure 1. The total

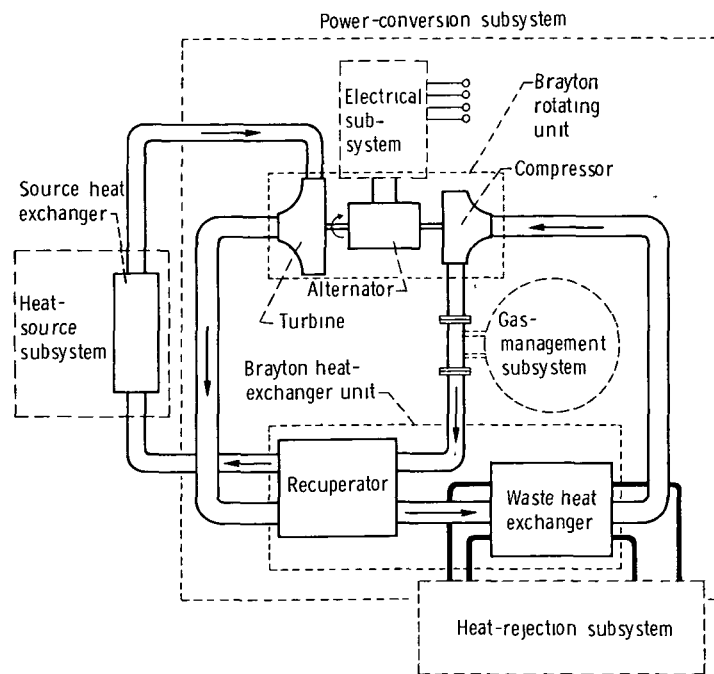


Figure 1. - Schematic diagram of Brayton cycle power system.

power system consists of the heat-source subsystem; the gas-filled, power-conversion subsystem; the liquid-filled, heat-rejection subsystem; and the electrical subsystem. Several heat sources may be used with the Brayton system. One presently being considered uses a radioisotope fuel.

The power-conversion subsystem is a closed loop which includes the Brayton Rotating Unit (BRU), the recuperator, and the waste heat exchanger. The working fluid is a mixture of helium and xenon. The molecular weight of this mixture is the same as that of Krypton (83.8). The turbine and compressor are single-stage, radial-flow machines. The alternator is a solid-rotor, modified Lundell-type generator. These three components are mounted on a common shaft which is supported by gas bearings. The BRU is designed to operate at a speed of 36 000 rpm.

The heat-rejection subsystem consists of the waste heat exchanger, cold plates, alternator cooling jacket, and radiator. The radiator rejects to space the unused cycle heat and the heat generated by losses in the electrical equipment.

The electrical subsystem provides for voltage regulation, BRU speed control, and overall engine control. The engine control system includes the automatic controls necessary to operate the system in a programmed manner for startup and shutdown. The Brayton power system is designed to deliver from 2 to 15 kWe (3 phase, 208/120 volts, 1200 Hz), depending on the heat-source power level and the system pressure level.

## COMPUTER SIMULATION

The simulation is a dynamic mathematical representation which integrates individual component models into a complete model of the Brayton system. This simulation provides the ability to study the response of the system to a wide variety of disturbances.

The symbols used in the simulation equations are defined in appendix A. A detailed description of the simulation is presented in appendix B. As input to the simulation, the alternator motoring torque was determined from tests performed on a prototype alternator (ref. 4). Typical motoring characteristics are shown in figures 2(a) and (b). These figures show the variation of torque and current with speed. These data were obtained for a frequency of 400 Hz and voltage-to-frequency ratios of 0.100, 0.075, and 0.050. Similar data were obtained for frequencies of 800 and 1200 Hz. Figures 3(a) and (b) show the variation of inrush current and locked-rotor torque with frequency. As would be expected, both inrush current and locked-rotor torque decrease as the voltage-to-frequency ratio is decreased.

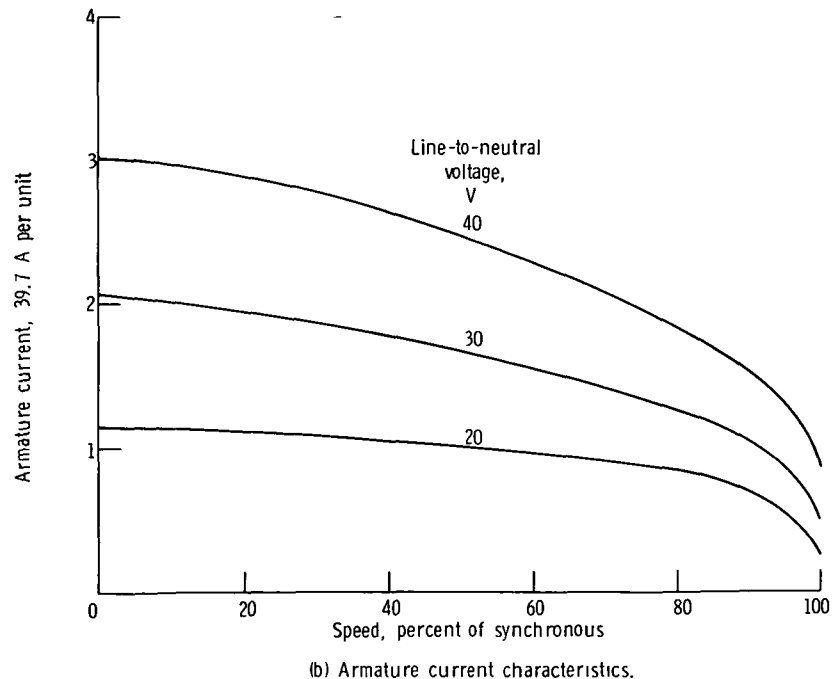
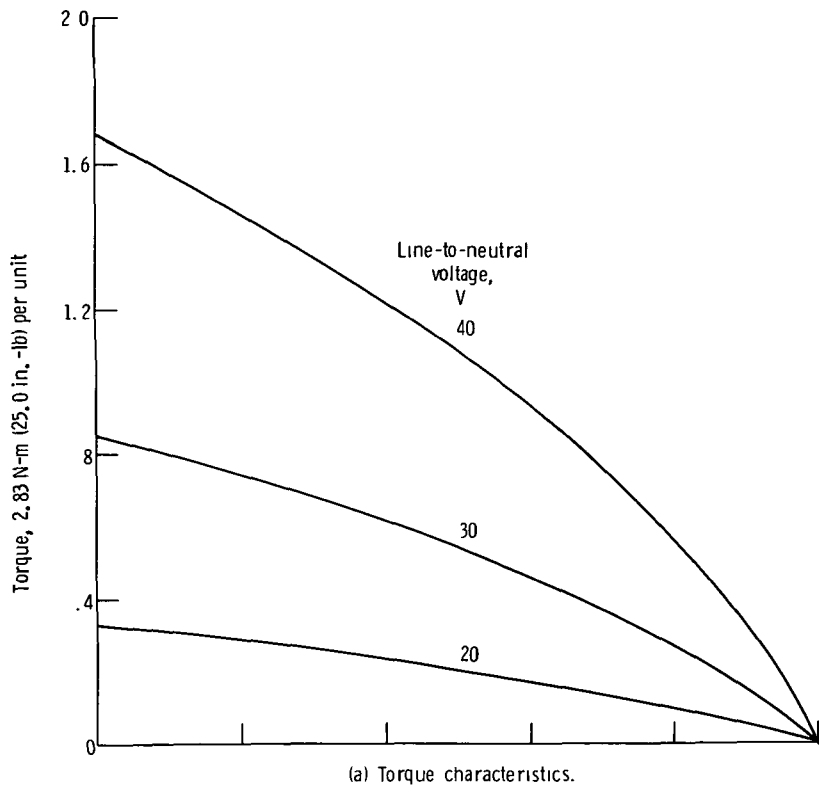
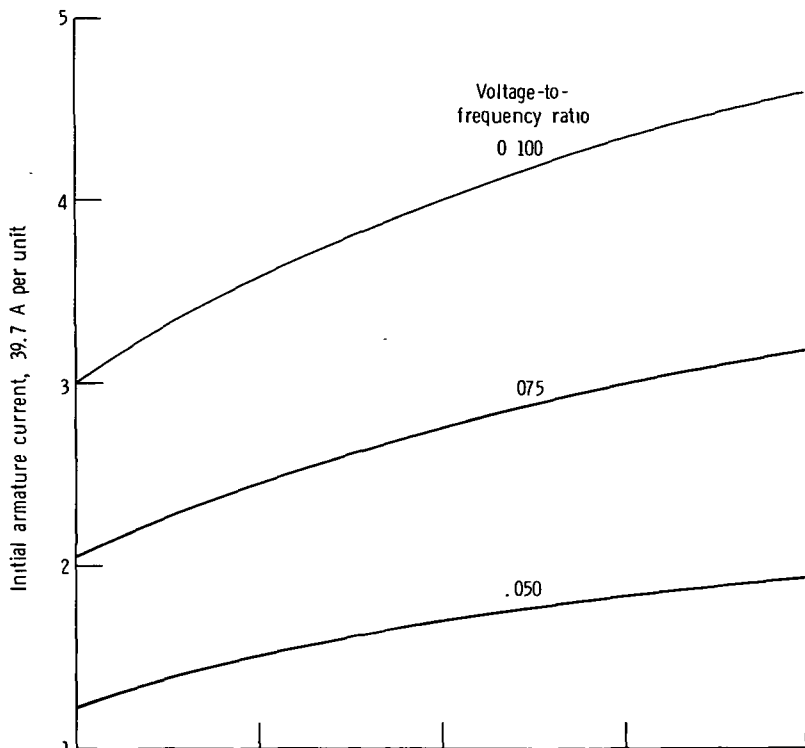
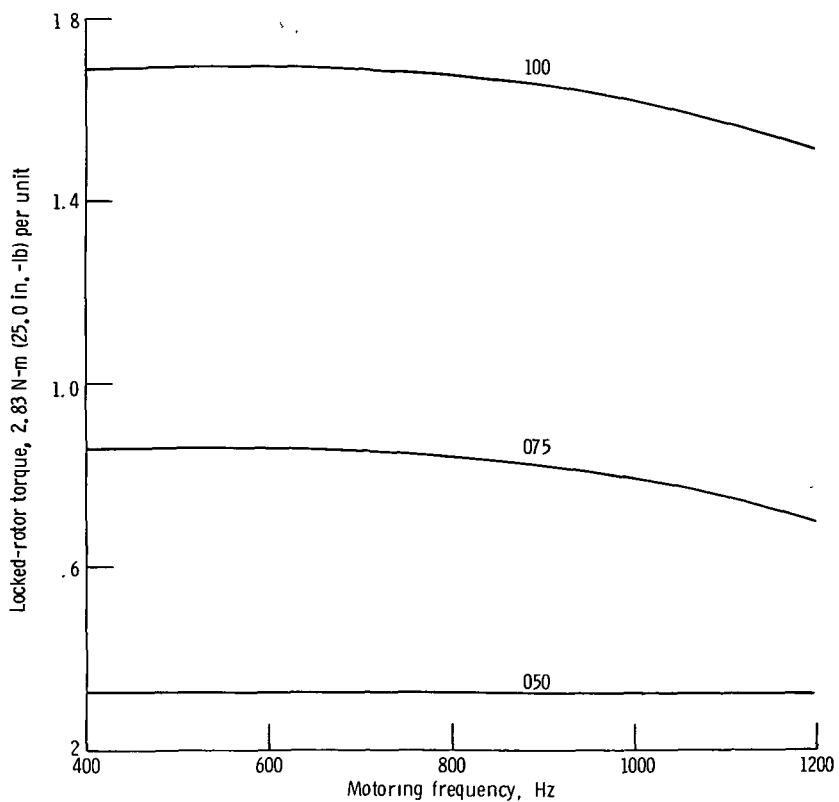


Figure 2. - Torque and armature-current characteristics of alternator no-load motor start. Test motoring frequency, 400 Hz; synchronous speed, 12 000 rpm.



(a) Initial armature current as a function of frequency.



(b) Locked-rotor torque as a function of frequency.

Figure 3 - Initial-armature-current and locked-rotor-torque characteristics of alternator no-load motor start Test motoring frequency, 400 Hz; synchronous speed, 12 000 rpm.

## STARTUP CONSIDERATIONS

Prior to system startup, the gas loop is filled with gas to a pressure level determined by the desired post-start operating power level. The motor start is then accomplished by applying a 3-phase ac voltage to the terminals of the alternator to drive it as an induction motor.

A motor start of the Brayton system consists of two steps: (1) motoring the alternator, and (2) bootstrap operation of the system to rated speed. The alternator is driven as a motor until near-synchronous speed is reached. At this point, the motoring source is disconnected, and if adequate turbine-inlet temperature has been reached by this time, the BRU achieves design speed by bootstrap operation. Three criteria which help to judge a motor startup are (1) armature current during motoring, (2) time to reach synchronous speed, and (3) time to reach design speed.

Armature current during motoring is shown in figures 2(b) and 3(a) for various voltages and frequencies. As shown in figure 2(b), for all voltages greater than 20 V, the current is above rated until at least 75 percent of synchronous speed is reached. To avoid overheating the alternator under these conditions, motoring time must be held to a minimum.

## RESULTS AND DISCUSSION

Motoring times determined from the analog simulation are shown in figure 4. This figure shows how motoring time (time to reach synchronous speed) varies with turbine-inlet temperature and voltage-to-frequency ratio. The prestart pressure level has little effect on motoring time. Figure 4(a) shows the variation of motoring time over a range of turbine-inlet temperatures from 800 K ( $1440^{\circ}$  R) to 1140 K ( $2060^{\circ}$  R). As temperature increases, motoring time decreases. Figure 4(b) shows the variation of motoring time over a range of voltage-to-frequency ratio of 0.050 to 0.100. As voltage-to-frequency ratio increases, motoring time decreases.

### Effects of System Parameters on Startup Time

Startup time is defined as the time required for the BRU to reach design speed. This time includes both motoring time and the bootstrap time. This total startup time will depend on motoring voltage and frequency, system prestart pressure, and turbine-inlet temperature. In actual system operation, the compressor-inlet temperature remains nearly constant during a system startup. For these studies, the compressor-inlet temperature was assumed to be at the design temperature of 300 K ( $540^{\circ}$  R).

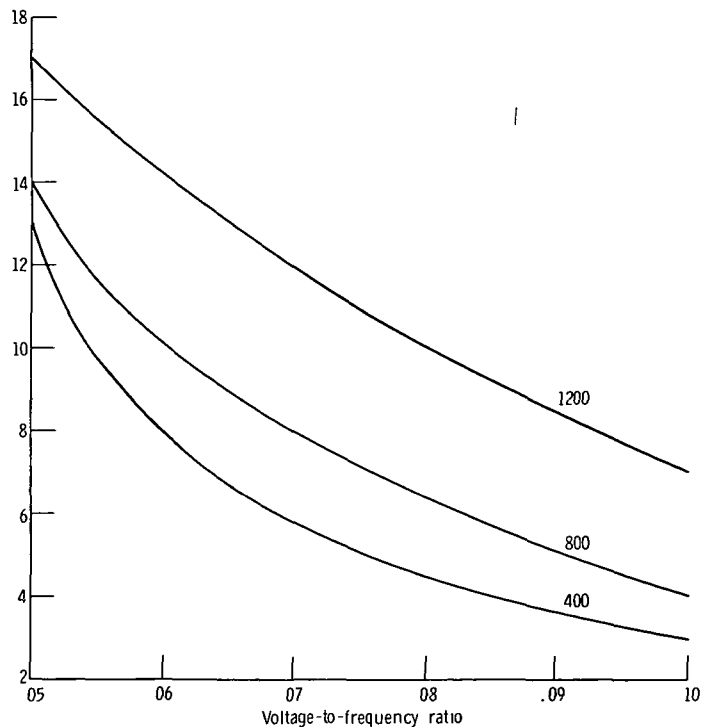
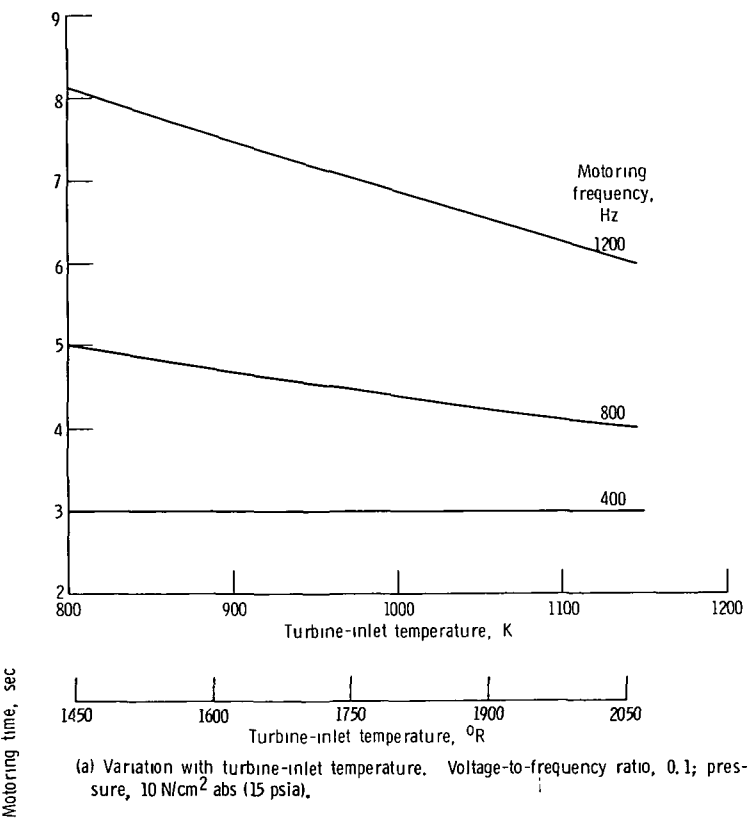


Figure 4 - Motoring time required to reach synchronous speed.

Turbine-inlet temperature. - Since the system is being designed for use with various heat sources, studies were made to determine the effect of turbine-inlet temperature on startup time. These results are shown in figure 5. The data shown are for a prestart pressure level of  $10 \text{ N/cm}^2$  abs (15 psia) and a voltage-to-frequency ratio of 0.10. As temperature decreases, startup time increases. This increase is a result of the decrease in turbine torque with decreasing turbine-inlet temperature. The 1200-Hz curve shows the least sensitivity to turbine-inlet temperature. Alternator torque is considerably larger than turbine torque during motoring. Since motoring at 1200 Hz brings the turbine to design speed, turbine-inlet temperature does not significantly affect startup time.

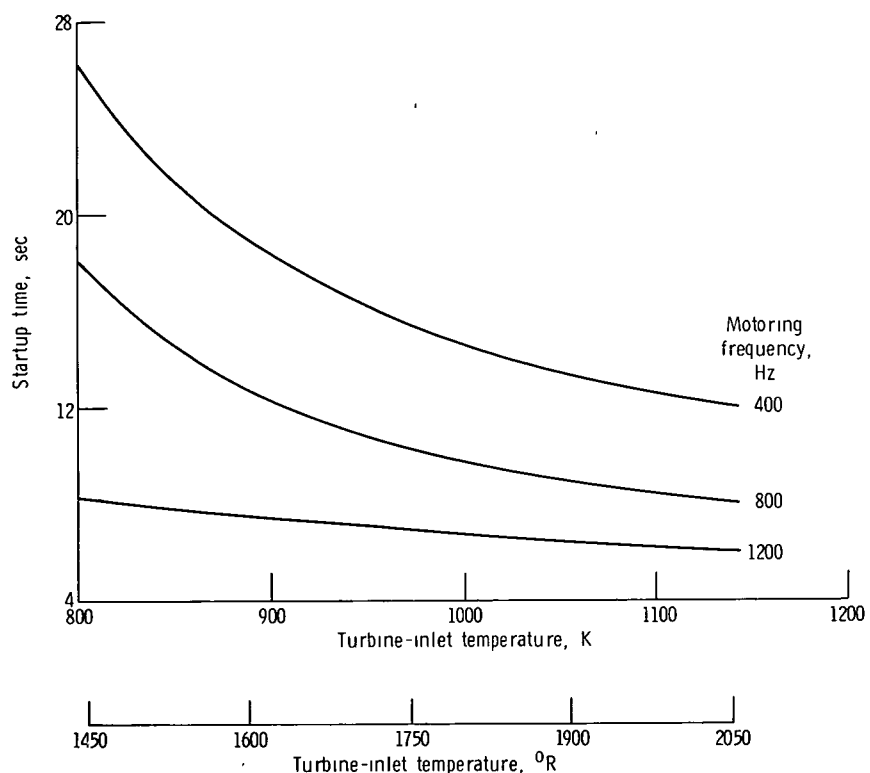


Figure 5. - Startup time as a function of turbine-inlet temperature. Voltage-to-frequency ratio, 0.1; pressure,  $10 \text{ N/cm}^2$  abs (15 psia).

Pressure level. - The prestart pressure level of the system will also affect startup time. It may be desirable to start the Brayton system with its rated inventory. Since the Brayton system is capable of a range of power outputs, there is a corresponding range of prestart pressure levels.

Prior to startup, the gas loop will contain its rated inventory, which, depending on the temperature and system piping configuration, will result in an initial gas-loop pressure.

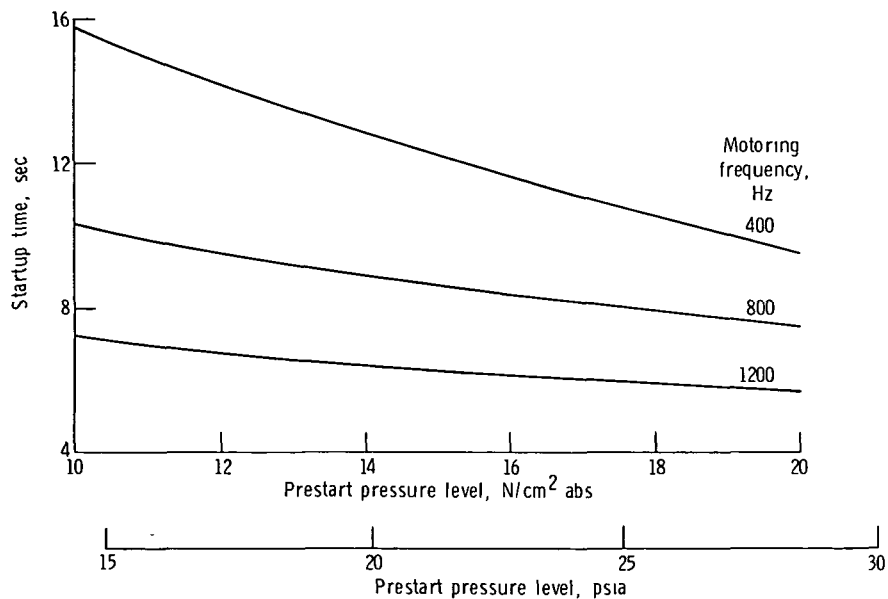


Figure 6. - Startup time as a function of prestart pressure level. Turbine-inlet temperature, 980 K ( $1760^{\circ}$  R); voltage-to-frequency ratio, 0.1.

The effect of pressure on startup time is shown in figure 6. These data are for a turbine-inlet temperature of 980 K ( $1760^{\circ}$  R) and a voltage-to-frequency ratio of 0.10. The 1200-Hz startups are least affected by pressure level.

Motoring frequency. - As has already been shown, frequency does have a direct effect on startup time. The motoring frequency determines synchronous speed and, therefore, the speed from which the BRU must bootstrap to design conditions. The amount of turbine torque is directly proportional to speed. This torque adds to the alternator torque available for acceleration. The sum of these torques then is greater for the higher motoring frequency. This effect is shown in figure 7 for a prestart pressure level of  $10 \text{ N/cm}^2 \text{ abs}$  (15 psia), a voltage-to-frequency ratio of 0.1, and various temperatures. As shown, total startup time varies inversely as motoring frequency. Turbine-inlet temperature does not significantly affect the 1200-Hz startups.

Voltage-to-frequency ratio. - The amount of alternator torque developed is directly related to the line current which, in turn, is related to the applied voltage. The effect of voltage on startup time is shown in figure 8. These data are for a prestart pressure level of  $10 \text{ N/cm}^2 \text{ abs}$  (15 psia) and a turbine-inlet temperature of 980 K ( $1760^{\circ}$  R). The data were obtained for voltage-to-frequency ratios ranging from 0.05 to 0.10. As shown in this figure, startup time increases as voltage decreases.

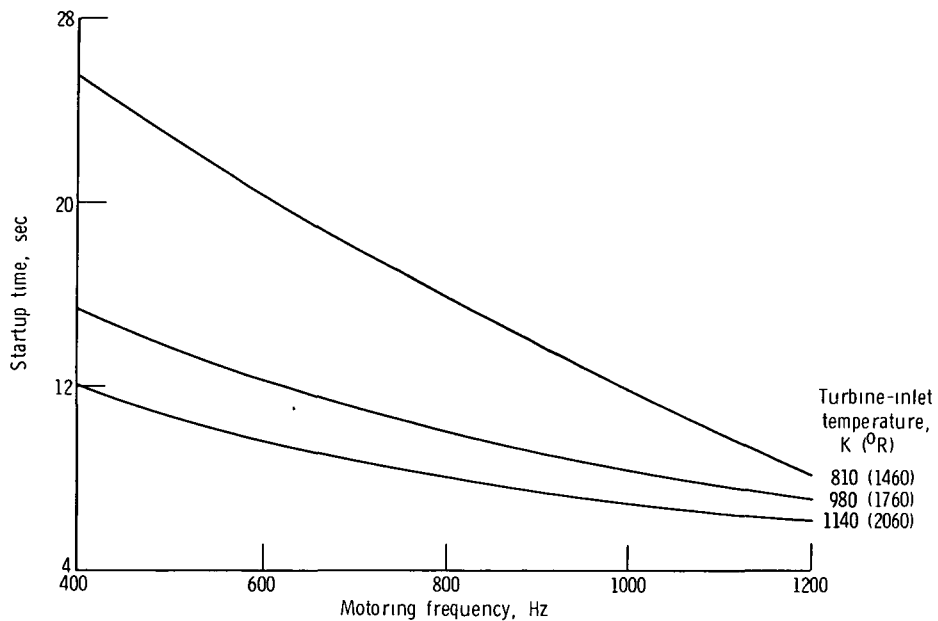


Figure 7 - Startup time as a function of motoring frequency Pressure level,  $10 \text{ N/cm}^2 \text{ abs}$  (15 psia); voltage-to-frequency ratio, 0.1.

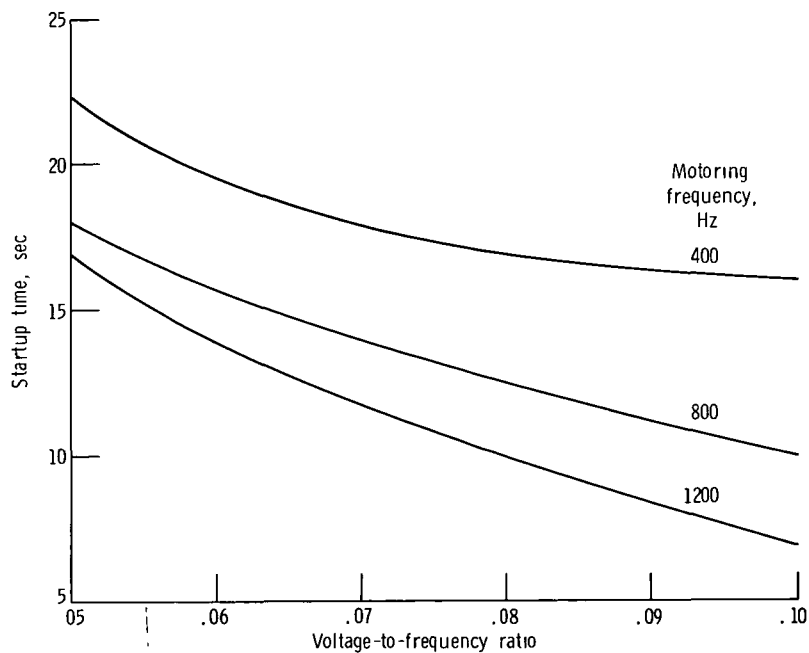


Figure 8 - Startup time as a function of voltage-to-frequency ratio. Pressure,  $10 \text{ N/cm}^2 \text{ abs}$  (15 psia); turbine-inlet temperature, 980 K (1760°R).

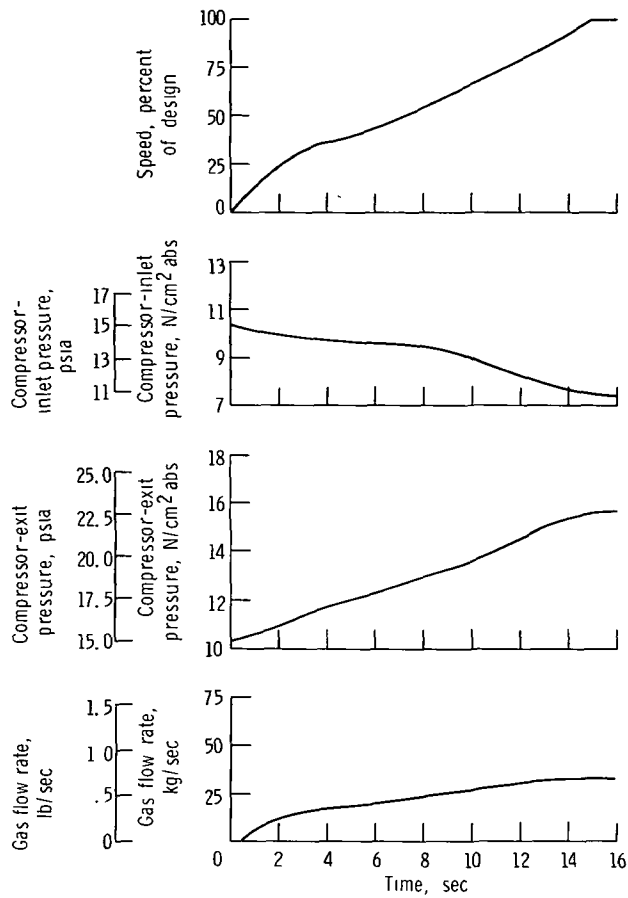


Figure 9 - Speed, pressure, and flow rate as functions of time for a typical startup. Pressure,  $10 \text{ N/cm}^2 \text{ abs}$  (15 psia); turbine-inlet temperature,  $980 \text{ K}$  ( $1760^\circ \text{ R}$ ); frequency, 400 Hz; voltage, 40 V

### Typical Motor Start

Parameters for a typical motor start are shown in figure 9. Plotted are the time responses of speed, pressures, and flow rate for a prestart pressure of  $10 \text{ N/cm}^2 \text{ abs}$  (15 psia), a turbine inlet temperature of  $980 \text{ K}$  ( $1760^\circ \text{ R}$ ), a frequency of 400 Hz, and a voltage of 40 V. Alternator motoring time is 3 seconds. Total startup time for these conditions is 15 seconds.

### CONCLUDING REMARKS

The analog computer studies have shown that motor starting the Brayton power system is possible over a wide range of system variables. Selection of particular motor-start variables (frequency, temperature, pressure, and voltage), therefore,

involves a tradeoff investigation based on operational limitations such as inverter complexity and battery size and weight.

The results of these studies show that startup time varies inversely as motoring frequency, voltage, turbine-inlet temperature, and prestart pressure level. An increase in any of these variables causes a decrease in startup time.

A typical Brayton system motor startup transient with a frequency of 400 Hz, a voltage-to-frequency ratio of 0.1, a prestart pressure of  $10 \text{ N/cm}^2$  abs (15 psia), and a turbine inlet temperature of 980 K ( $1760^\circ \text{ R}$ ) required 3 seconds of alternator motoring and 12 seconds of bootstrap operation to achieve design speed, which is well within system design limits.

Lewis Research Center,  
National Aeronautics and Space Administration,  
Cleveland, Ohio, September 17, 1971,  
112-27.

## APPENDIX A

### SYMBOLS

$A$	heat transfer area, $\text{m}^2$ ; $\text{ft}^2$	$T_{\text{out}}, T$	turbine-exit temperature, K; ${}^{\circ}\text{R}$
$C_{\text{cold}}$	$WC_p$ of cold fluid, $\text{J}/(\text{sec})(\text{K});$ $\text{Btu}/(\text{sec})({}^{\circ}\text{R})$	$T_q$	torque, N-m; in.-lb
$C_{\text{hot}}$	$WC_p$ of hot fluid, $\text{J}/(\text{sec})(\text{K});$ $\text{Btu}/(\text{sec})({}^{\circ}\text{R})$	$T_1$	temperature at liquid outlet of heat exchanger, K; ${}^{\circ}\text{R}$
$C_{\text{max}}$	larger $WC_p$ , $\text{J}/(\text{sec})(\text{K});$ $\text{Btu}/(\text{sec})({}^{\circ}\text{R})$	$T_2$	temperature at liquid inlet of heat exchanger, K; ${}^{\circ}\text{R}$
$C_{\text{min}}$	smaller $WC_p$ , $\text{J}/(\text{sec})(\text{K});$ $\text{Btu}/(\text{sec})({}^{\circ}\text{R})$	$T_3$	temperature at gas outlet of heat exchanger, K; ${}^{\circ}\text{R}$
$C_p$	specific heat, $\text{J}/(\text{sec})(\text{K});$ $\text{Btu}/(\text{sec})({}^{\circ}\text{R})$	$T_4$	temperature at gas inlet of heat exchanger, K; ${}^{\circ}\text{R}$
$E_{\text{ff}}$	effectiveness, dimensionless	$T_5$	temperature at hot inlet of recuperator, K; ${}^{\circ}\text{R}$
$I$	polar moment of inertia, $\text{kg}\cdot\text{m}\cdot$ $\text{sec}^2$ ; in.-lb-sec $^2$	$T_6$	temperature at hot outlet of recuperator, K; ${}^{\circ}\text{R}$
$K$	pressure-drop constant, $\text{m}^2/\text{sec};$ $\text{in.}^2/\text{sec}$	$T_7$	temperature at cold inlet of recuperator, K; ${}^{\circ}\text{R}$
$N$	rotational speed, rpm	$T_8$	temperature at cold outlet of recuperator, K; ${}^{\circ}\text{R}$
$\text{NTU}$	number of heat-transfer units, $UA/C_{\text{min}}$ , dimensionless	$t$	time, sec
$P$	pressure, $\text{N}/\text{cm}^2$ abs; psia	$U$	overall heat conductance, $\text{J}/(\text{sec})(\text{K})(\text{m}^2); \text{Btu}/(\text{sec})({}^{\circ}\text{R})(\text{ft}^2)$
$R$	gas constant of helium-xenon mixture, $30.5 (\text{N})(\text{m})/(\text{kg})(\text{K});$ $18.4 (\text{ft})(\text{lbf})/({}^{\circ}\text{R})(\text{lbm})$	$V$	volume, $\text{m}^3$ ; $\text{ft}^3$
$S$	Laplace transform variable	$W$	mass flow rate, kg/sec; lb/sec
$T$	temperature, K; ${}^{\circ}\text{R}$	$\tau$	time constant, sec
$T_{\text{in}, C}$	compressor-inlet temperature, K; ${}^{\circ}\text{R}$	$\tau_1$	300 sec
$T_{\text{in}, T}$	turbine-inlet temperature, K; ${}^{\circ}\text{R}$	$\tau_2$	10 sec
$T_{\text{out}, C}$	compressor-exit temperature, K; ${}^{\circ}\text{R}$		

500 sec  
20 sec  
500 sec  
20 sec  
3 sec

$\tau_8$       3 sec  
Subscripts:  
alt      alternator  
C      compressor  
T      turbine

## APPENDIX B

### ANALOG COMPUTER SIMULATION

The analog computer simulation of the Brayton power system has three dynamic variables of interest: (1) pressure, (2) speed of Brayton Rotating Unit (BRU), and (3) temperature. These variables are continuously calculated by the computer and can be used to predict the response of the system to a wide variety of disturbances. The simulation contains all of the equations necessary to define the system operation. Extensive use is also made of diode function generators to simulate the three-variable turbine and compressor maps.

#### Pressure and BRU Speed Dynamics

To dynamically simulate the loop pressures, the Brayton system is divided into two volume lumps, as shown in figure 10. The pressure for each lump is calculated by using the equation

$$P = \frac{TR}{V} \int (W_{in} - W_{out}) dt \quad (B1)$$

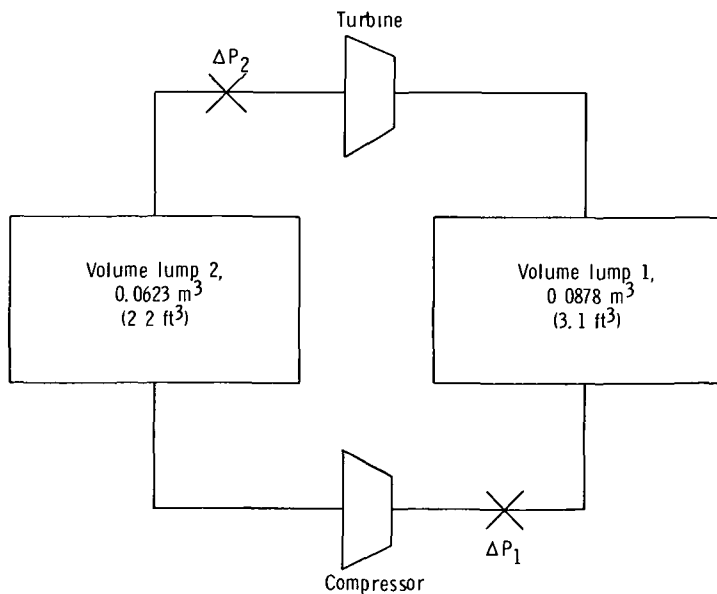


Figure 10. - Gas volume distribution for simulation of Brayton system

where  $P$ ,  $T$ , and  $V$  are the pressure, temperature, and volume, respectively, of the volume lump under consideration,  $R$  is the gas constant  $30.5 \text{ (N)(m)/(kg)(sec)}$  ( $18.4 \text{ (ft)(lbf)/(lbm)}^{\circ}\text{R}$ ) for the helium-xenon mixture, and  $W$  is the gas flow rate. The temperature used here is the weighted average of the temperatures throughout the lump. These pressures calculated for the two volume lumps represent the turbine and compressor discharge pressures. To account for the distributed pressure losses, the calculation

$$\Delta P = K \frac{W^2}{P} \quad (\text{B2})$$

is made. These pressure losses are subtracted from the volume pressures and the results are then used as the turbine and compressor inlet pressures. From these equations, the pressures at the inlet and discharge of both the turbine and the compressor are determined. Knowing these pressures, the pressure ratios,  $P_{\text{out}}/P_{\text{in}}$ , for the turbine and compressor are determined. Pressure ratio is used as one input into the turbine and compressor maps (ref. 5). The other inputs to the maps are inlet temperature, inlet pressure, and BRU speed.

BRU speed is determined by equating the sum of the torques acting on the shaft to the shaft dynamics.

$$T_{q,T} - T_{q,C} - T_{q,\text{alt}} = (2\pi I) \frac{dN}{dt} \quad (\text{B3})$$

where  $T_{q,T}$  is the turbine driving torque,  $T_{q,C}$  is the compressor torque, and  $T_{q,\text{alt}}$  is the torque available to the alternator before losses. The representative losses are windage, bearing, thermal, and electromagnetic. The windage and bearing losses are assumed to vary with speed squared, while thermal and electromagnetic losses are assumed constant. These losses are subtracted from the gross alternator power to yield net electrical power.

$$\text{Power (kW)}_{\text{net}} = 1.15 \times 10^{-5} N T_{q,\text{alt}} - \text{Power (kW)}_{\text{losses}} \quad (\text{B4})$$

Along with speed, pressure ratio, and inlet pressure, the gas flow rate and torque for the turbine and compressor may be obtained from experimental maps if inlet temperature is known.

## Temperature Dynamics

For the studies reported herein, both heat-source-outlet and radiator-outlet temperatures were held constant at various values. Therefore, there are no dynamics associated with these temperatures. The major heat-transfer components in the system, other than the heat source and radiator, are the gas-to-liquid waste heat exchanger and the gas-to-gas recuperator. The inlet and outlet temperatures of these components, as well as the outlet temperatures of the turbine and compressor, are calculated.

Waste heat exchanger. - Since the radiator is not included in the simulation, the dynamic response of the liquid side of the heat exchanger is not considered. The only temperature of interest is the gas-outlet temperature. Its steady-state temperature is calculated from the basic equation for a counterflow heat exchanger:

$$E_{ff} = \frac{C_{hot}(T_4 - T_3)}{C_{min}(T_4 - T_2)} \quad (B5)$$

where  $T_4$  is the gas-inlet temperature,  $T_3$  is the gas-outlet temperature, and  $T_2$  is the liquid-inlet temperature. The effectiveness  $E_{ff}$  of the heat exchanger is given by the equation

$$E_{ff} = \frac{1 - \exp \left[ -NTU \left( 1 - \frac{C_{min}}{C_{max}} \right) \right]}{1 - \frac{C_{min}}{C_{max}} \exp \left[ -NTU \left( 1 - \frac{C_{min}}{C_{max}} \right) \right]} \quad (B6)$$

Therefore, the gas-outlet temperature  $T_3$  can be calculated if the design of the heat exchanger, the mass flow rates, and the inlet temperatures are known. However, this gives only the steady-state temperature. To include the dynamics in the simulation, a 100-lump digital computer model was programmed to determine the heat-exchanger response. The response of gas-outlet temperature  $T_3$  was found for changes in gas inlet-temperature  $T_4$  and liquid-inlet temperature  $T_2$ . The response to changes in  $T_4$  and  $T_2$  were approximated by first-order time lags with time constants  $\tau_1$  and  $\tau_2$ , respectively. The final equation for the gas outlet temperature is

$$T_3(S) = \frac{T_4(S)}{\tau_1 S + 1} - \frac{C_{min} E_{ff}}{C_{hot}} \left( \frac{T_4(S)}{\tau_1 S + 1} - \frac{T_2(S)}{\tau_2 S + 1} \right) \quad (B7)$$

Recuperator. - The recuperator is modeled in the same manner as the gas-to-liquid heat exchanger. However, for the recuperator the flow rates and specific heats on both sides of the heat exchanger are the same. Therefore, the equations for recuperator effectiveness are

$$E_{ff} = \frac{T_8 - T_7}{T_5 - T_7} \quad (B8)$$

$$E_{ff} = \frac{T_5 - T_6}{T_5 - T_7} \quad (B9)$$

where  $T_8$  is the cold-outlet temperature,  $T_7$  is the cold-inlet temperature,  $T_5$  is the hot-inlet temperature, and  $T_6$  is the hot-outlet temperature.

To include the recuperator dynamics, a digital computer model was again programmed, and a first-order response was matched to the results. The final equations for the outlet temperatures of the recuperator are

$$T_8(S) = \frac{T_7(S)}{\tau_3 S + 1} + E_{ff} \left( \frac{T_5(S)}{\tau_4 S + 1} - \frac{T_7(S)}{\tau_3 S + 1} \right) \quad (B10)$$

$$T_6(S) = \frac{T_5(S)}{\tau_5 S + 1} - E_{ff} \left( \frac{T_5(S)}{\tau_5 S + 1} - \frac{T_7(S)}{\tau_6 S + 1} \right) \quad (B11)$$

Thus, if the mass flow rates (for determining effectiveness) and the inlet temperatures are known, the outlet temperatures can be calculated.

Turbomachinery. - The outlet temperatures of the turbine and compressor are functions of inlet temperature and the power put into or taken from the gas. A first-order response was included in the temperature calculation to include the dynamics associated with the heat capacity of the machinery scrolls, wheels, and housing. The following equations were used to calculate the outlet temperatures:

$$T_{out, T} = \frac{T_{in, T}}{\tau_7 S + 1} - \frac{1.15 NT_{q, T}}{WC_p} \times 10^{-5} \quad (B12)$$

$$T_{out, C} = \frac{T_{in, C}}{\tau_8 S + 1} + \frac{1.15 NT_{q, C}}{WC_p} \times 10^{-5} \quad (B13)$$

## REFERENCES

1. Klann, John L.: Steady-State Analysis of a Brayton Space-Power System. NASA TN D-5673, 1970.
2. Cantoni, Dennis A.; and Thomas, Ronald L.: Analog Computer Studies of a 2 to 10 Kilowatts Electric Brayton Cycle Space Power System Including Startup and Shutdown. Proceedings of the 4th Intersociety Energy Conversion Engineering Conference. AIChE, 1969, pp. 668-678.
3. Gilbert, L. J.; Curreri, J. S.; and Cantoni, D. A.: Motor Starting Techniques for the 2- to -15 kw Brayton Space Power System. NASA TM X-67819, 1971.
4. Repas, David S.; and Frye, Robert J.: Motor-Starting Characteristics of a Modified Lundell Alternator. NASA TM X-2200, 1970.
5. Nusbaum, William J.; and Kofskey, Milton G.: Cold Performance Evaluation of 4.97-Inch Radial-Inflow Turbine Designed for Single-Shaft Brayton Cycle Space-Power System. NASA TN D-5090, 1969.